SYNERGISTIC EFFECT OF GROUND GRANULATED BLAST FURNACE SLAG AND RICE HUSK ASH ON PROPERTIES OF REACTIVE POWDER CONCRETE

SREENATH SREEKUMARAN*, SARAVANA RAJA MOHAN KALIYAPERUMAL
School of Civil Engineering, SASTRA Deemed University, Thanjavur, Tamilnadu, India – 613 401

Reactive Powder Concrete (RPC) mixes consume a very high volume of cement in which a part only can undergo hydration due to the adoption of a very low water to binder (W/B) ratios. The unhydrated part of cement can act as a filler in the mixes. In this study, for the sustainable development of RPC mixes, the filler part of cement was replaced with Ground Granulated Blast furnace Slag (GGBS). Further reactive Rice Husk Ash (RHA) was introduced to the mix as a replacement for inert Quartz Powder (QP) filler to bring in a better pozzolanic activity. Flow characteristics of the mixes were evaluated. Compressive strength of the mixes was also evaluated. For the optimization of results, regression models were established based on Box-Behnken method of Experiment Design. Sustainability Indicators such as Embodied Energy (EE) and Embodied Carbon (EC) of the mixes were also evaluated. It was observed that flow of the mixes was improved considerably due to the addition of GGBS and got reduced due to the incorporation of RHA. Improved strength was observed up to 30% replacement of cement with GGBS. For all the cases, 100% replacement of QP with RHA lead to better strength results. Further, EE and EC of mixes were considerably reduced due to the incorporation of GGBS and RHA.

Keywords: *Reactive Powder Concrete, Rice Husk Ash, Response Surface Design, Embodied Energy, Embodied Carbon*

1. Introduction

Over the decades, many investigations are being performed targeting the attainment of better strength and durability of cementitious composites. Reactive Powder Concrete (RPC) is one of such advancements. The basic concept of RPC was first envisaged by Richard and Cheyrezy in the early 1990s [1]. Incorporation of ultrafine cementitious materials such as Silica Fume (SF) and fine fillers such as Quartz Powder (QP) helped in the achievement of the dense microstructure of RPCs. The adoption of lower water to binder (W/B) ratios is another aspect of RPC, which will help in attaining maximum strength. High range water reducers were used at higher volumes to maintain the workability to the level of self-compaction, even at the lower W/B ratios [2]. Usage of fibers to reinforce the matrix helped in attaining better compressive strength, flexural strength, modulus of elasticity, and ductility. The incorporation of fibers will further help in the inhibition of crack propagation [3,4].

Self-compacting nature, high strength, and durability characteristics of RPC make it suitable for special applications such as overlaying airfield pavements, construction of ductile joints in bridge decks, etc. RPCs offer a high compressive strength in the range of 120-800 MPa and tensile strength in the rage of 20-150 MPa. The density of RPCs ranges from 2500-3000 kg/m^3.

RPCs usually consume a large amount of cement which is in the range of 800-1000 kg/m^3[5,6]. However, thermogravimetry investigations reveal that, as the water-binder ratios employed are smaller, only a portion of the used cement is participating in hydration. Between 40-60% of the used cement only is getting hydrated [7]. The unhydrated cement will serve as a filler to help the microstructure become more dense. As the manufacturing process of cement causes 7-9 % of global CO_2 emission [8], the use of high amount of cement is not desirable. Hence, the replacement of a part of cement, with a suitable substitute, is essential. Ground Granulated Blast-furnace Slag (GGBS) is a by-product generated from the steel production units and is a proven Supplementary Cementitious Material (SCM) [6]. Kim et al. concluded their study, stating that GGBS can improve the flowability of Ultra-High-Performance Concrete (UHPC) without compromising strength [9]. In this study, GGBS was used as a partial replacement of cement.

SF is an essential constituent material for RPC, which brings in outstanding mechanical and durability characteristics [10], and QP is considered as an ideal filler for RPC mixes [1,11]. The functions of SF in the RPC mixes are the filling of voids, improving the flowability, and production of the secondary hydrates [12]. Tuan et al. studied the possibility of using Rice Husk Ash (RHA) instead of SF in UHPC mixes. The authors observed significant improvement in the strength of UHPC mixes as a result of the incorporation of RHA [10]. Unlike SF, QP will remain inert unless the mixes are subjected to heat treatments for curing [13]. Heat treatment of concrete is practicable in the production of the pre-cast elements, but, for the in-situ applications, normal water curing is feasible. It would be advantageous if the inert QP can be replaced with suitable reactive filler, which can undergo pozzolanic activity even under low

*Author corespondent/*Corresponding author*,
E-mail: sreenath@civil.sastra.ac.in

Table 1

Chemical Properties of Materials - XRF Results

Oxide	CaO	SiO_2	Al_2O_3	MgO	SO_3	Fe_2O_3	Na_2O	K_2O
Cement	63.23	24.63	6.76	2.19	1.54	0.53	0.44	0.68
GGBS	43.10	32.40	15.70	6.62	1.61	0.48	0.23	0.54
SF	0.29	98.70	0.29	0.11	0.03	0.03	-	88 PPM
QP	0.01	99.50	0.08	0.01	-	0.04	-	-
RHA	0.49	95.64	0.07	0.62	0.18	0.05	0.15	1.01

Table 2

Physical Properties of Materials

Property	Cement	GGBS	SF	QP	RHA	RS
Specific Gravity	3.15	2.85	2.29	2.65	2.25	2.62
Bulk Density (g/cc)	1.14	1.09	0.60	1.28	0.20	1.88

temperatures. It has been found that RHA has physical and chemical properties comparable to QP. Considering the ability of RHA to undergo reaction even at the ambient temperature, this study is meant to observe the effect of replacement of QP with RHA on the fresh and hardened properties of RPC mixes. As the combined effect of hydration of GGBS and RHA in RPC is less explored, this study is destined to optimize the mixes modified by replacing cement with GGBS and QP with RHA. The workability of modified mixes was evaluated for different W/B ratios. Further, the compressive strength of the mixes was also assessed. Scanning Electron Microscopy (SEM) analysis was done to ascertain the refinement of microstructure due to the synergistic action of GGBS and RHA.

Particle packing methods are widely used for the formulation of mix proportions of RPCs [14]. The mixes with high packing density are expected to possess maximum strength and durability characteristics. The highly sophisticated test methods and analyses carried out for the characterizations of ultrafine particles make particle packing method of optimization of RPC mixes least feasible for in-situ applications. Probabilistic modeling is a proven method for the optimization of concrete mix proportions [15,16]. In this study, for the optimization of flow and strength characteristics of RPC mixes, the Design of Experiments (DoE) was done, and regression models were developed. The models developed can be used as a tool for the design of RPC mixes of the same kind. Further, ecological parameters such as Embodied Energy (EE) and Embodied Carbon (EC) were also evaluated. These parameters are indicators of the sustainability of the mixes.

2. Research Significance

Most of the published researches have focused on the solo effect of GGBS and RHA on properties of RPCs. The synergistic effect of these materials is a least explored area. In this study, the combined effect of GGBS and RHA on properties of RPCs have been studied. Further, in this study, regression models have been developed for the optimization of flow and strength properties of modified RPCs.

3. Materials and methodology

3.1 Material Properties

Typical RPC mix is constituted with hydraulic cement, SF, inert quartz powder (QP), super-plasticizer (SP), water, and steel fibers. Ordinary Portland Cement (OPC) of 53 Grade conforming to IS 12269 [17] was used in this study. Silica Fume of particle size between 0.04 μm and 20 μm and with Silicon dioxide (SiO_2) content of 95.64% was used to compose the binder phase of the mixes. GGBS with limited impurity and of average particle size 45 μm was also used as a supplementary cementitious material. Natural river sand (RS) of particle size ranges from 150 μm to 2.36 mm was the fine aggregate used. Sand used was in Saturated Surface Dry (SSD) condition. QP, which is hydrophilic in nature and of particles passing through 75 μm sieve was used as a supplementary filler. Rice Husk Ash (RHA) was used for the partial or full replacement of QP was also of particles passing through 75 μm sieve. The physical and chemical properties of the materials are detailed in **Tables 1 and 2**.

Using fine powders as binding materials and the adoption of a lower W/B ratio will lead to a decrease in the flowability of the mixes. For overcoming this, polycarboxylate ether-based High Range Water Reducer (HRWR) was used as SP. Crimped steel fibers of diameter 0.45 mm, length 12.5 mm, and tensile strength 1800 MPa were used for reinforcing the matrix.

3.2 Mix Proportion

As there are no comprehensive methods available for the proportioning of RPC mixes, several trial mixes were made with reference to the proportions discussed in recent research articles [18,19]. The technique of proportioning of RPC mixes based on particle packing theory is efficient but delicate and not easily performable in real-life problems. In this study, based on the frequently adopted proportions, particle size ranges for the constituents were fixed. Constituent materials were sieved to segregate particles to the prefixed sizes.

The control mix for this study was prepared with OPC, SF, RS, QP, water, SP, and steel fibres.

Table 3

Mix proportions

Mix ID	OPC (kg/m^3)	SF (kg/m^3)	GGBS (kg/m^3)	RS (kg/m^3)	QP (kg/m^3)	RHA (kg/m^3)	SP (L/m^3)
M1	960	144	-	1017	115	-	34
M2	864	144	96	1017	115	-	34
M3	768	144	196	1017	115	-	34
M4	672	144	288	1017	115	-	34
M5	576	144	384	1017	115	-	34
M6	960	144	-	1017	57.5	57.5	34
M7	864	144	96	1017	57.5	57.5	34
M8	768	144	196	1017	57.5	57.5	34
M9	672	144	288	1017	57.5	57.5	34
M10	576	144	384	1017	57.5	57.5	34
M11	960	144	-	1017	-	115	34
M12	864	144	96	1017	-	115	34
M13	768	144	196	1017	-	115	34
M14	672	144	288	1017	-	115	34
M15	576	144	384	1017	-	115	34

Note: The above-specified mixes were prepared for three different W/C ratios such as 0.17 (163 L/m^3), 0.2 (192 L/m^3), and 0.23 (221 L/m^3). As a whole, 45 mixes were made for the experimental analysis. All the mixes are reinforced with 2% by volume of concrete.

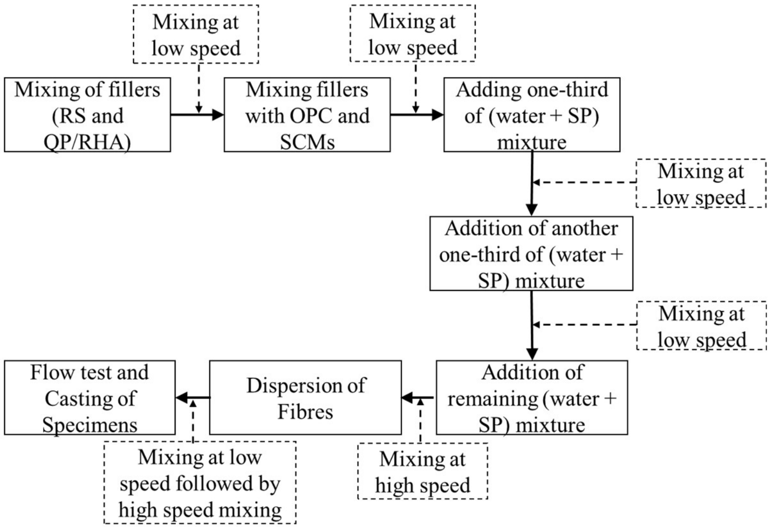

Fig. 1 - Flow chart describing the mixing process

The mix was then modified by replacing OPC with GGBS (10, 20, 30, and 40% by mass of cement) and QP with RHA (50 and 100% by mass of QP). Mixes were prepared with three different W/B ratios, such as 0.17, 0.20, and 0.23. A total number of 45 mixes were prepared. The details of the proportioned mixes are described in **Table 3**.

3.3 Mixing, Specimen Preparation and Curing

High shear mixing of the constituents was done in a planetary mixer. Dry mixes of all constituent powders were made first, to which the mixture of the required amount of water and SP was added at three different stages. **Fig. 1** is a chart explaining the workflow of mixing. Cube molds of size 70.7 mm were arranged for the casting of specimens for the compressive strength test. No mechanical compaction was done while casting the specimens as the mixes are expected to be compacted by itself.

All the specimens were kept in molds for 24 hours after casting under the room temperature. During this period, specimens were covered with polythene membranes to avoid the evaporation of water. Specimens made of each mix were cured in water for 28 days.

3.4 Testing methods

Flow table test as recommended in ASTM C1437 [20] was conducted to evaluate the workability of mixes. Compressive strength test was carried out on specimens conforming to IS 516 [21] on Compression Testing Machine (CTM) of capacity 3000 kN. Further, morphology of the mixes was assessed with the aid of SEM.

3.5 Statistical Design of Experiments and Mix Optimisation

Statistical designs of experiments are techniques which will help in developing precise numerical models and thereby in the optimization of responses with a minimum number of trials and errors. In this study, Box-Behnken Design (BBD)

Table 4

Levels of independent parameters

Parameter	Lowest Level	Median Level	Highest level
X1: GGBS Content (% by mass of PC)	0	20	40
X2: RHA (% by volume of QP)	0	50	100
X3: W/B ratio	0.17	0.20	0.23

Table 5

Random tests performed

Runs	Coded Values			Percentage by Mass				W/B (X_3)
	A	B	C	PC	QP	GGBS (X_1)	RHA (X_2)	
R1	0	1	-1	80	0	20	100	0.17
R2	-1	1	0	100	0	0	100	0.20
R3	-1	-1	0	100	1	0	0	0.20
R4	0	0	0	80	0.5	20	50	0.20
R5	0	0	0	80	0.5	20	50	0.20
R6	0	1	1	80	0	20	100	0.23
R7	-1	0	-1	100	0.5	0	50	0.17
R8	0	-1	1	80	1	20	0	0.23
R9	0	-1	-1	80	1	20	0	0.17
R10	1	1	0	60	0	40	100	0.20
R11	1	0	1	60	0.5	40	50	0.23
R12	0	0	0	80	0.5	40	50	0.20
R13	1	-1	0	60	1	40	0	0.20
R14	-1	0	1	100	0.5	0	50	0.23
R15	1	0	-1	60	0.5	40	50	0.17

method of Response Surface design was performed to assess the effect of three independent parameters, such as the GGBS content (X_1), RHA content (X_2), and W/B ratio (X_3) on the responses of fresh and hardened RPC mixes. The evaluated responses were the flow diameter (Y_1) and the compressive strength of RPC mixes (Y_2). Non-linear Model Analysis of Variance was done to evaluate the influence of control parameters on responses with minimal error variance. The general expression which describes the response surfaces can be as given in Eq. 1.

$$Y = f(X_1, X_2, X_3) \quad (1)$$

In this study, for BBD, three distinct levels of each independent parameter, such as the lowest, median, and highest values were considered. The levels of control parameters considered in this study are provided in the **Table 4**.

The coded variables were obtained using the Eq. 2.

$$x_i = \frac{X_i - X_0}{\Delta X} \quad \text{---- (2)}$$

Where x_i is the coded variable, X_i is the process variable, and ΔX is the change in the un-coded value of the variable.

To evaluate the relation between the process variables and the response variables, a second-order equation, as described in Eqn. 3, is assumed.

$$y = C_0 + \sum_{i=1}^{k} C_i X_i + \sum_{i=1}^{k} C_{ii} X_i^2 + \sum_{i=1}^{k} \sum_{j>1}^{k} C_{ij} X_i X_j + \varepsilon \quad (3)$$

Where C_0, C_i, C_{ii}, and C_{ij} are the regression coefficients. The coefficient C_0 is defined for the intercept, C_i for the linear term, C_{ii} for the quadratic term, and C_{ij} for the interaction term. X_i and X_j are the independent variables, and k is the number of independent variables in the study. ε represents the random error in the evaluated responses.

Analysis of Variance (ANOVA) was performed to assess the significance of differences between various samples, and thereby the regressions coefficients were estimated. The summary of fit at a significance level of 95% ($P \le 0.05$) was obtained. The fitness of the developed quadratic equation was established by observing the Coefficient of Determination (R^2).

Totally fifteen random tests (including three central runs) were performed with the different levels of the variables as described in **Table 5**. **Fig. 2** is a schematic representation of the adopted BBD. The coded values were varying as -1 to 0 to 1, which represents the lowest, median, and highest values of the variables.

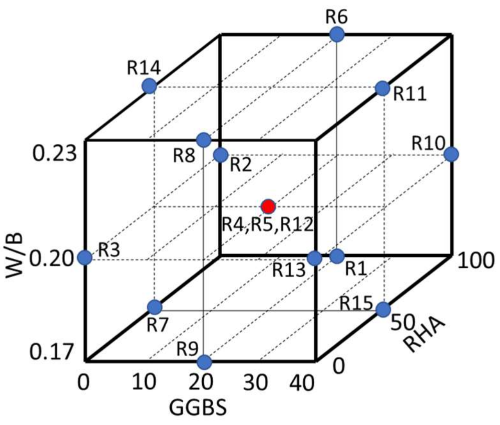

Fig. 2 - Schematic diagram of the adopted Box-Behnken design

reduction in the workability of mixes. The mixes with 100% RHA exhibited considerably low improvement in the flow percentages such as 5.42%, 4.76% and 6.51% for W/B ratios 0.17, 0.20 and 0.23 respectively.

The addition of spherical GGBS particles and their effective dispersion due to high shear mixing led to the improvement in flow. In addition, the poor (slow) hydration of GGBS also contributed to the improvement in flow [22,23]. In contrast, addition of RHA lead to the reduction in flow. Reduction in the flow is the effect of porous nature, high specific surface area and rough surface texture of RHA particles [10]. In addition, RHA will initially absorb the mixing water and the same will be stored

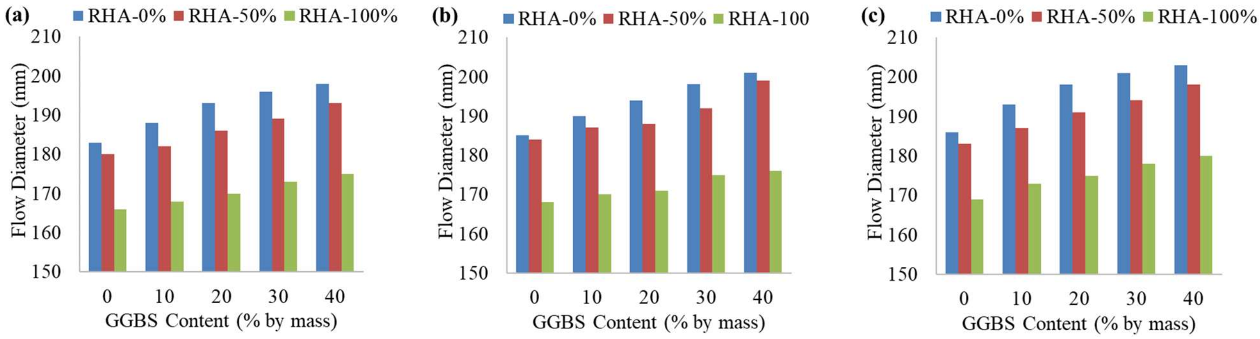

Fig - 3 Results of flow test: (a) for W/B ratio = 0.17; (b) for W/B ratio = 0.20; (c) for W/B ratio = 0.23.

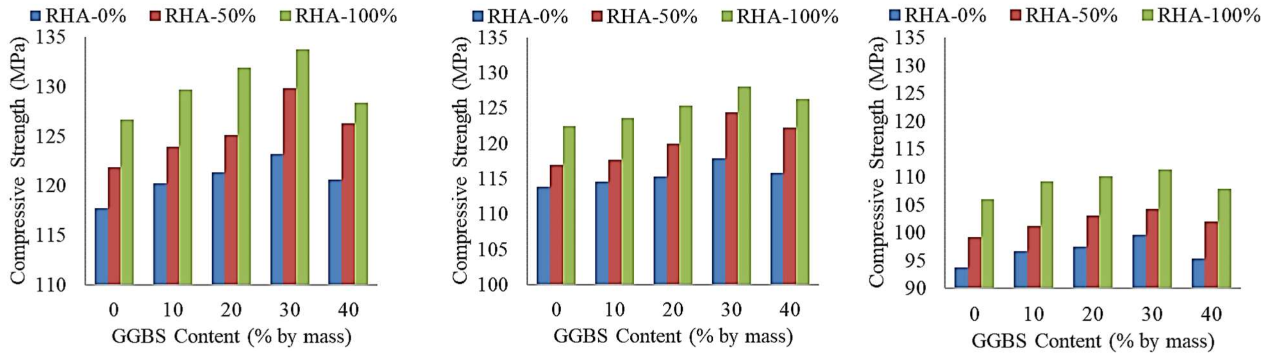

Fig. 4. Results of compression test: (a) for W/B ratio = 0.17; (b) for W/B ratio = 0.20; (c) for W/B ratio = 0.23.

4. Results and Discussions

4.1 Experimental Results

4.1.1 Flow Characteristics

The flow values of different mixes are plotted in the **Fig. 3**. Considerable improvement in the flow was observed as the cement in the mix was replaced with GGBS. However, the improvement has got diminished to some degree due to the replacement of QP with RHA.

Compared to the control mixes with 0% GGBS, the flow of mixes with 0% RHA and 40% GGBS was improved by 8.19%, 8.64% and 9.14% for W/B ratios 0.17, 0.20 and 0.23 respectively. For the mixes with 50% RHA, the comparative improvement was 7.22%, 8.15% and 8.19% for W/B ratios 0.17, 0.20 and 0.23 respectively. Further replacement of QP with RHA showed significant

in the pores. This will lead to the reduction in effective W/B ratio in the initial stages of mixing and there by the reduction in workability [24,25]. Also, it was noted that, even for prolonged mixing time, the dispersion of RHA particles was poor. This is due to the low density of RHA. The improper dispersion is also a reason for inferior workability of mixes with higher RHA content.

4.1.2 Compressive strength

The variation of compressive strength values with varying GGBS content, RHA content and W/B are plotted in the **Fig. 4.**

Among the specimens, the results exhibited by the mixes made by replacing 30% OPC with GGBS and 100% QP with RHA were superior. Replacement of OPC with GGBS beyond 30% lead to reduction in strength. The maximum strength results observed were 133.76, 128.03, and 111.36 MPa for the W/B ratios 0.17, 0.20, and 0.23, respectively. The strength of the mixes with W/B ratios 0.17 and 0.2 were improved by 13.59% and 8.73% compared to the reference mix (mix with 100% OPC, and 100% QP). The strength of the mix with W/B ratio 0.23 was diminished by 5.42% compared to the reference mix.

For all the mixes, the incorporation of SF and steel fibers helped in attaining better compressive strength. Improved strength was exhibited by the mixes modified with GGBS. The well-dispersed ultrafine GGBS particles can fill the pores effectively and thereby densifies the granular structure. Pozzolanic reaction of GGBS produces additional Calcium Silicate Hydrate(C-S-H) gel which also has become the reason for improved strength [18].

Addition of RHA is also a reason for the improved strength. RHA imbibes a part of the mixing water in the initial stage, which reduced the effective W/B ratio and thereby improved strength of the mixes. The stored water is used for the internal curing at the later ages. The reactive silica in RHA and the stored water undergoes pozzolanic reaction in the presence of Calcium Hydroxide to form additional C-S-H gel [24,25].

However, a reduction in compressive strength was exhibited by the mixes with more than 30% of cement replaced with GGBS. The drop in strength is due to the occurrence of low-density C-S-H gel produced by GGBS. It can also be due to the deficiency in free calcium hydroxide for pozzolanic reaction [23].

4.1.3 Morphology of RPC mixes

The Fig. 5 shows the SEM images of the control mix and that of the mix which showed higher compressive strength (mix with 30% GGBS and 100% RHA).

From the SEM images of the control mix and the mix which showed the higher strength, it is evident that, the microstructure of the concrete became finer due to the addition of GGBS and RHA. It was observed that micropores were considerably less in the matrix of the mix with 30% GGBS and 100% RHA. This is a clear indication of the pozzolanic activity of GGBS and RHA. The matrix was refined and became denser due to the addition of these pozzolans and as a result, the strength was improved.

4.2 Probabilistic Assessment of Results

The optimization of results was done by designing the experiments in the Box-Behnken method. A significance level of 0.05 was adopted in all the cases to assess the effect of constraints such as GGBS content (X_1), RHA content (X_2), and W/B ratio (X_3) on the workability and compressive strength of the mixes. The estimated responses were the flow diameter (Y_1), and compressive strength (Y_2), and these were considered as the dependent variables. The relationships between dependent and independent variables are second-order non-linear polynomial equations in the form expressed below.

$$Y_i = k_0+k_1X_1+k_2X_2+k_3X_3+k_4X_1^2+k_5X_2^2+k_6X_3^2+ +k_7X_1X_2 + k_8X_1X_3+k_9X_2X_3 \quad \text{----(4)}$$

Where $k_1,k_2\ldots\ldots k_9$ are the coefficients for the response functions and are computed using non-linear regression analysis.

4.2.1 Flow values

The results of ANOVA for flow percentages are detailed in **Table 6(a)**. Based on the regression coefficients, the relation between significant variables and flow percentage can be expressed as given by Eqn. 5. The equation is in uncoded units.

$$Y_1 = 217.8 + 0.308\, X_1 + 0.0200\, X_2 - 386\, X_3 - 0.00125\, X_1{*}\, X_1 - 0.002000\, X_2{*}\, X_2 + 1111\, X_3{*}\, X_3 - 0.002000\, X_1{*}\, X_2 + 0.833\, X_1{*}\, X_3 + 0.000\, X_2{*}\, X_3 \quad \text{---(5)}$$

From the Table 6(a), it is evident that all the linear terms have significant effect on the flow percentage as their P-values are less than 0.05 at 95% significant level. Among the square terms, except that of RHA content, the other two were insignificant in predicting the flow diameters as their P-values were greater than 0.05 at 95% significant level. Only the interaction term between GGBS and

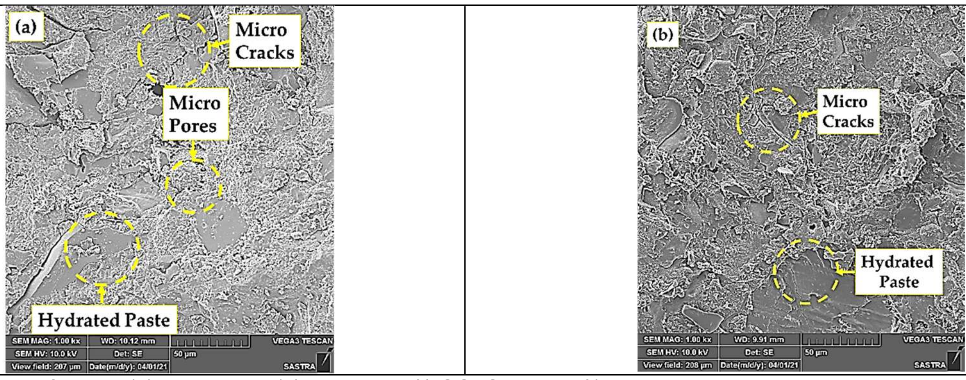

Fig. 5 - Morphology of mixes; (a) control mix; (b) mix with 30% GGBS and 100% RHA

Table 6 (a)

Results of ANOVA for flow diameters

Source	DF	Adj SS	Adj MS	F-Value	P-Value
X_1	1	338.00	338.000	375.56	0.000
X_2	1	968.00	968.000	1075.56	0.000
X_3	1	40.50	40.500	45.00	0.001
X_1* X_1	1	0.92	0.923	1.03	0.358
X_2* X_2	1	92.31	92.308	102.56	0.000
X_3* X_3	1	3.69	3.692	4.10	0.099
X_1* X_2	1	16.00	16.000	17.78	0.008
X_1* X_3	1	1.00	1.000	1.11	0.340
X_2* X_3	1	0.00	0.000	0.00	1.000
Total Error	5	4.50	0.900		
R^2	98.86 %				
R^2-Adjusted	96.80 %				

Table 6(b)

Results of ANOVA for compressive strength

Source	DF	Adj SS	Adj MS	F-Value	P-Value
X_1	1	20.58	20.58	38.75	0.002
X_2	1	223.66	223.66	421.19	0.000
X_3	1	1075.78	1075.78	2025.86	0.000
X_1* X_1	1	9.75	9.75	18.36	0.008
X_2* X_2	1	5.70	5.70	10.73	0.022
X_3* X_3	1	132.70	132.70	249.90	0.000
X_1* X_2	1	0.78	0.78	1.47	0.279
X_1* X_3	1	0.76	0.76	1.43	0.286
X_2* X_3	1	1.07	1.07	2.02	0.215
Total Error	5	2.66	0.53		
R^2	99.82 %				
R^2-Adjusted	99.50 %				

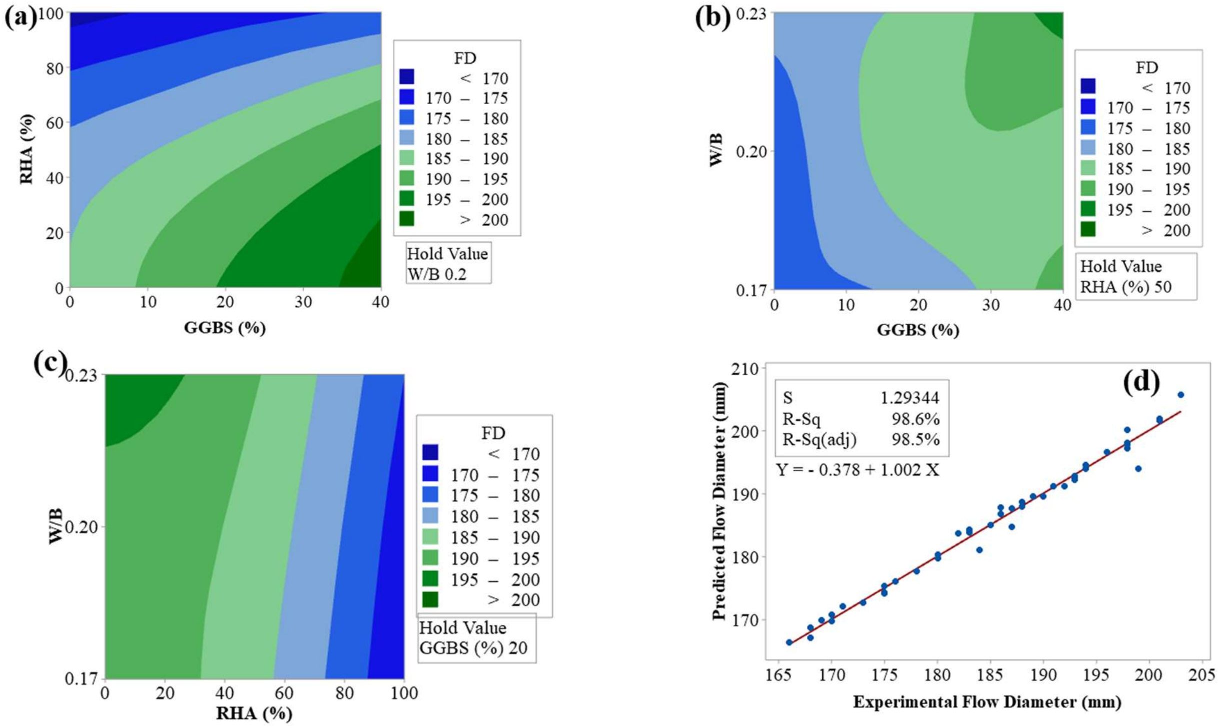

Fig. 6 - Effect of interaction between independent variables in the determination of flow diameters: (a) GGBS Content Vs RHA Content; (b) GGBS Content Vs W/B; (c) RHA Content Vs W/B; (d) Fitted Line Plot

RHA was significant for the statistical assessment of flow results. Contour plots in the **Fig. 6** details the effects of the mix parameters on the flow diameters of the mixes.

The fitted line plot in **Fig. 6(d)** describes the statistical relationship between the experimental flow values and those predicted in RSM. Higher R^2 indicates the competency of the model in predicting the flow values.

4.2.2 Compressive strength

ANOVA results for compressive strength specimens are detailed in **Table 6(b)**. Based on the regression coefficients, the relation between significant variables and compressive strength of the specimens can be expressed as given by Eqn. 6. The equation is in uncoded units.

$$Y_2 = -75.4 + 0.366 X_1 - 0.0218 X_2 + 2275 X_3 - 0.004063 X_1{*}X_1 + 0.000497 X_2{*}X_2 - 6661 X_3{*}X_3 + + 0.000443 X_1{*}X_2 - 0.725 X_1{*}X_3 + 0.345 X_2{*}X_3 \quad (6)$$

From **Table 6(b),** it is clear that the linear and square terms of all the independent variables are significant in predicting the compressive strength of the specimens as the P-values are less than 0.05 at 95% significance level. None of the interaction terms were significant, since the P-values were greater than 0.05 at the significance level of 95%.

Contour plots in the **Fig. 7** describes the effects of the mix parameters on the compressive

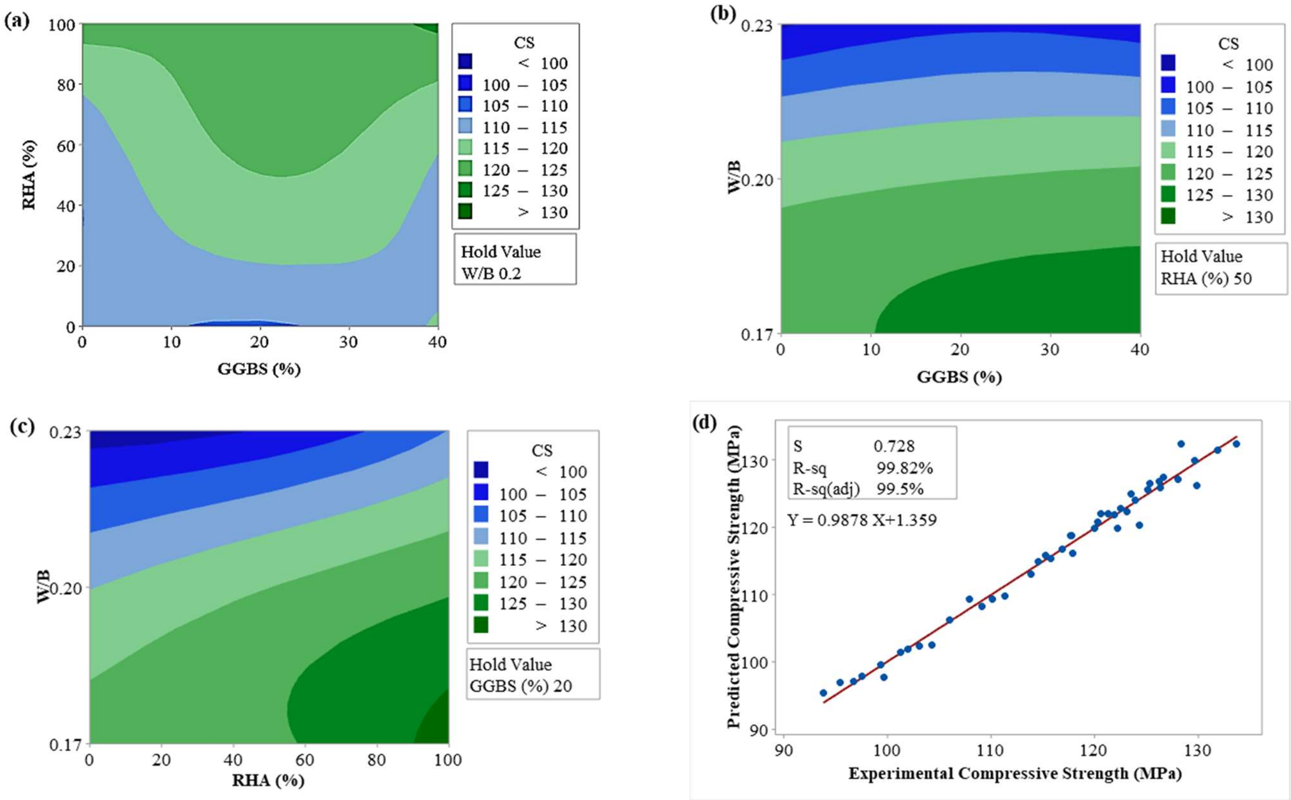

Fig. 7 - Effect of interaction between independent variables in the determination of compressive strength (a) GGBS Content Vs RHA Content; (b) GGBS Content Vs W/B; (c) RHA Content Vs W/B; (d) Fitted Line Plot

strength of specimens. The fitted line plot in **Fig. 7(d)** describes the statistical relationship between the experimental compressive strength of specimens and those predicted in RSM. Higher R^2 value of 99.5% indicates the competency of the model in predicting the compressive strength of the mixes.

5. Assessment of Sustainability

The sustainability of the mixes is assessed based on CO_2 emission and energy demand. Global Warming Potential (GWP) of any material, which is governed by the quantity of CO_2 emitted, and energy demand for the production, has socio-economic impacts [26]. Estimation of the Embodied Energy [EE] and Embodied Carbon [EC] of mixes is based on several assumptions and reports of similar researches. **Table 7** provides the details of EE and EC of the constituent of materials used in this study. As the embodied energy and carbon of water is negligible, the variation in W/B ratio is not considered for the assessment. Table 10 provides the values of estimated impact per cubic meter of fifteen typical mixes (Ref. Table 3)

As a quantification of the sustainability of mixes, two parameters, such as S_E and S_c, are defined as presented in Eqn. 7 and Eqn. 8 [33].

$$S_E = \frac{\text{Embodied Energy of mix (MJ/m}^3\text{)}}{\text{Compressive Strength (MPa)}} \quad \text{---- (7)}$$

$$S_C = \frac{\text{Embodied Carbon of mix (kg CO}_2\text{/m}^3\text{)}}{\text{Compressive Strength (MPa)}} \quad \text{---- (8)}$$

Where S_E is the Embodied Energy Parameter (MJ/m^3.MPa) and S_C is the Embodied Carbon Parameter (kg.CO_2/ m^3.MPa)

Table 7

EE and EC of constituent materials

Material	EE (MJ/kg)	EC ($kgCO_2$/kg)	References
OPC	3.939	0.830	[27]
GGBS	0.939	0.0625	[28]
SF	0.036	0.014	[29]
RS	0.081	0.0051	[30]
QP	0.850	0.020	[30]
RHA	-0.353	0.157	[31]
SP	35.000	1.500	[32]
Water	Negligible	Negligible	
Steel Fibres	36.000	2.830	[30]

Among the developed concretes, those with a W/B ratio of 0.17 exhibited maximum strength. The strength results of these mixes are considered for the evaluation of sustainability parameters. Estimated parameters of the modified mixes are compared with those of the control mix. Lower values of these parameters compared to the control mix indicate the enhanced sustainability of the mixes. The values of sustainability parameters of fifteen typical mixes also are detailed in Table 8.

Table 8

Embodied energy and carbon of mixes

Mix. No.	EE (MJ/m^3)	EC ($kgCO_2/m^3$)	S_E ($MJ/m^3.MPa$)	S_C ($kg.CO_2/ m^3.MPa$)
M1	10837.6	1303.9	92.0	11.1
M2	10541.1	1229.6	87.6	10.2
M3	10244.6	1155.4	84.4	9.5
M4	9947.3	1081.1	80.8	8.8
M5	9650.8	1006.8	80.0	8.3
M6	10768.4	1311.8	88.3	10.8
M7	10471.9	1237.5	84.5	9.9
M8	10175.5	1163.3	81.3	9.3
M9	9878.1	1088.9	76.1	8.4
M10	9581.6	1014.7	75.9	8.0
M11	10699.2	1319.6	84.5	10.4
M12	10402.8	1245.4	80.2	9.6
M13	10106.3	1171.1	76.6	8.9
M14	9808.9	1096.8	73.3	8.2
M15	9512.5	1022.6	74.1	7.9

From **Table 8** it is clear that the control mix M1 (0% GGBS and 0% RHA) has a higher energy demand of 10837.6 MJ/m^3. The mix M11 (0% GGBS and 100% RHA) exhibited higher carbon emission of 1319.6 $kgCO_2/m^3$. Considerable reduction in the energy demand and carbon emission can be observed as the incorporation of GGBS and RHA modifies the mix. The mix M15 (40% GGBS and 100% RHA) showed the minimum energy demand of 9512.5 $MJ/m^{3,}$ which is 12.22% less than that of control mix. And the mix M5 (40% GGBS and 0% RHA) exhibited minimum carbon emission of 1006.8 $kgCO_2/m^{3,}$ which is 22.78% less than that of control mix. Further, the mix M14 showed the least values of S_E as 73.3 $MJ/m^3.MPa$, whereas the mix M15 exhibited the least S_E value of 7.9 $kg.CO_2/ m^3.MPa$. The lowest values of these parameters indicate the better sustainability of the mix.

According to the analysis results, GGBS can be considered as a potential substitute for OPC in RPCs. The use of GGBS helped in enhancing sustainability by reducing the energy demand for the production of RPC and by reducing the resulting carbon emission. The results also indicate the ability of RHA to enhance strength and to reduce the environmental impact of RPC mixes.

6. Summary and Conclusions

Based on the observations made in the experimental program, statistical analysis and assessment of sustainability, the following conclusions can be drawn.

1. Significant improvement in the workability of RPC mixes was observed due to the addition of GGBS. This effect can be attributed to the morphology (smooth spherical particles) and poor hydration of GGBS particles, and better dispersion of GGBS occurred due to high shear mixing.
2. A considerable reduction in the workability of RPC mixes was observed due to the addition of RHA. The absorption of the mixing water in the initial stages due to the porous nature of RHA is the prime reason for this. This can also be ascribed to the morphology (rough-surfaced angular shaped particles) of RHA.
3. Maximum strength observed was at the level of 30% GGBS and 100% RHA, for all the three W/B ratios. This ascertains the ability of GGBS to act as a SCM for the development of RPC. This also shows the potential of RHA to act as a reactive filler.
4. The higher R^2 values of the regression models indicate the competency of Box-Behnken design in predicting the workability and compressive strength of RPC mixes. Higher composite desirability value of the optimization function and lower error percentages of the optimization results also is proof for the efficiency of the model.
5. The incorporation of GGBS and RHA in the mixes helped in reducing the energy demand as well as the carbon emission. Hence, GGBS can be considered as a potential SCM, and RHA can be used as an able reactive filler for the sustainable production of RPCs.

Acknowledgement

The authors would like to acknowledge the Vice-Chancellor of SASTRA Deemed University, Thanjavur, for the encouragement given and for providing facilities to carry out the research.

REFERENCES

[1] P. Richard and M. Cheyrezy, Composition of reactive powder concretes, Cement and Concrete Research, 1995, **25**, 1501.

[2] N. M. Azmee and N. Shafiq, Ultra-high-performance concrete: From fundamental to applications, Case Studies in Construction Materials, 2018, 9, e00197.

[3] P. Balaguru, R. Narahari and M. Patel, Flexural toughness of steel fibre reinforced concrete, ACI Materials Journal, 1992, **89**(6), 541.

[4] N. Banthia and JF. Trottier, Concrete reinforced with deformed steel fibres. Part II: Toughness characterization, ACI Materials Journal, 1995, **92**(2), 146. (5,6)
[5] P. Richard and M. H. Cheyrezy, Reactive powder concretes with high ductility and 200–800 MPa compressive strength, ACI SP144-24, 1994, **144**, 507.
[6] Y. Halit, Y. Y. Mert, Y. Huseyin, A. Serdar and T. Selcuk, Mechanical properties of reactive powder concrete containing high volumes of ground granulated blast furnace slag, Cement and Concrete Composites, 2010, **32**, 639.
[7] Marcel Cheyrezy, Vincent Maret and Laurent Frouin, Microstructural anlysis of RPC (Reactive Powder Concrete), Cement and Concrete Research, 1995, **25**, 1491.
[8] P. J. M. Monteiro, S. A. Miller and A. Horvath, Towards sustainable concrete, Nature Materials, 2017, 16 (7), 698.
[9] Heeae Kim, Taehoon Koh and Sukhoon Pyo, Enhancing flowability and sustainability of ultra-high performance concrete incorporating high replacement levels of industrial slags, Construction and Building Materials, 2016, **123**, 153.
[10] N. Van Tuan, G. Ye, K. van Breugel and O. Copuroglu, Hydration and microstructure of ultra-high performance concrete incorporating rice husk ash, Cement and Concrete Research, 2011, **41**, 1104.
[11] Sung-Hoon Kang, Ji-Hyung Lee, Sung-Gul Hong and Juhyuk Moon, Microstructural investigation of heat-treated ultra-high-performance concrete for optimum production, Materials, 2017, **10**(9), 1106.
[12] D. D. L. Chung, Review: Improving cement-based materials by using silica fume, Journal of Materials Science, 2002, **37**, 673.
[13] Parameshwar N. Hiremath and Subhash C. Yaragal, Effect of different curing regimes and durations on early strength development of reactive powder concrete, Construction and Building Materials, 2017, **154**, 72.
[14] R. Yu, P. Spiesz and H. J. H. Brouwers, Mix design and properties assessment of Ultra-High Performance Fibre Reinforced Concrete (UHPFRC), Cement and Concrete Research, 2014, **56**, 29–39.
[15] Parthiban Kathirvel and Saravana Raja Mohan Kaliyaperumal, Probabilistic modeling of geopolymer concrete using response surface methodology, Computers and Concrete, 2017, 19(6), 737.
[16] K. A. Soudki, E. F. El-Salakawy and N. B. Elkum, Full factorial optimization of concrete mix design for hot climates, Journal of Materials in Civil Engineering, 2001, 13, 427.
[17] IS 12269:2013, Ordinary Portland Cement, 53 Grade Specification, BIS, New Delhi, India.
[18] P. Ganesh and A. Ramachandra Murthy, Tensile behaviour and durability aspects of sustainable ultra-high-performance concrete incorporated with GGBS as cementitious material. Construction and Building Materials, 2019, **197**, 667.
[19] Davood Mostofinejad, Mojtaba Rostami Nikoo and Seyed Arman Hosseini, Determination of optimized mix design and curing conditions of reactive powder concrete (RPC), Construction and Building Materials, 2016, **123**, 754. (27)
[20] ASTM C1437, Standard Test Method for Flow of Hydraulic Cement Mortar, ASTM, Philadelphia, PA, 2015.
[21] IS 516:1959, Methods of Test for Strength of Concrete. BIS, New Delhi.
[22] J. M. A, Megat, J.J. Brooks, K. Shahid and R. Patrice, Influence of supplementary cementitious materials on engineering properties of high strength concrete, Construction and Building Materials, 2011, 25, 2639.
[23] O. Erdogan, E. Mustafa and I. D. Halil, Utilization and efficiency of ground granulated blast furnace slag on concrete properties – a review, Construction and Building Materials, 2016, 105, 423–434.
[24] V.-T.-A. Van, C. Rößler, D.-D. Bui and H.-M. Ludwig, Rice husk ash as both pozzolanic admixture and internal curing agent in ultra-high-performance concrete, Cement and Concrete Composites, 2014, **53**, 270.
[25] K. Wille, A. E. Naaman and G. J. Parra-Montesinos, Ultra-high-performance concrete with compressive strength exceeding 150 MPa (22 ksi): a simpler way, ACI Materials Journal, 2011, **108**, 46.
[26] Gettu, R., et al., Sustainability assessment of cements and concretes in the Indian context: influence of supplementary cementitious materials. In Proceedings of the fourth international conference on sustainable construction materials and technologies, Las Vegas, USA, 2016, edited by Ghafoori, N., Claisse, P., Ganjian, E., Naik, T.R., p. 1142.
[27] Sanoop Prakasan, Sivakumar Palaniappan and Ravindra Gettu, Study of Energy Use and CO2 Emissions in the Manufacturing of Clinker and Cement, Journal of The Institution of Engineers (India): Series A, 2020, **101**, 221.
[28] R. Gettu, A. Patel, V. Rathi, S. Prakasan, A. S. Basavaraj, S. Palaniappan and S. Maity, Influence of supplementary cementitious materials on the sustainability parameters of cements and concretes in the Indian context, Materials and Structures, 2019, **52**(10).
[29] Job Thomas, Nassif Nazeer Thaickavil and T. N. Syamala, Supplementary Cement Replacement Materials for Sustainable Concrete, edited by H. Drück, R. G. Pillai, M. G. Tharian and A. Z. Majeed, Green Buildings and Sustainable Engineering, Springer Transactions in Civil and Environmental Engineering, Springer Nature, Singapore, 2019, p. 387.
[30] Geoffrey Hammond and Craig Jones, A BSRIA Guide, Embodied Carbon, The inventory of carbon and energy (ICE), edited by Fiona Lowrie and Peter Tse, Old Bracknell Lane West, Bracknell, Berkshire, UK, 2011.
[31] Lingling Hu, Zhen He and Shipeng Zhang, Sustainable use of rice husk ash in cement-based materials: Environmental evaluation and performance improvement, Journal of Cleaner Production, 2020**, 264**, 121744.
[32] R. Ranade, Ph.D. thesis, Advanced Cementitious Composite Development for Resilient and Sustainable Infrastructure, University of Michigan, 2014.
[33] Rui Xiao, Yuetan Ma, Xi Jiang, Miaomiao Zhang, Yiyuan Zhang, Yanhai Wang, Baoshan Huang d and Qiang He, Strength, microstructure, efflorescence behavior and environmental impacts of waste glass geopolymers cured at ambient temperature, Journal of Cleaner Production, 2020, **252**, 119610.

****